

Coexisting *on-* and *off-center* Yb^{3+} sites in $\text{Ce}_{1-x}\text{Yb}_x\text{Fe}_4\text{P}_{12}$ skutterudites

F. A. Garcia¹, D. J. Garcia², M. A. Avila¹, J. M. Vargas¹, P. G. Pagliuso¹, C. Rettori¹,
M. C. G. Passeggi³, S. B. Oseroff⁴, P. Schlottmann⁵, B. Alascio², and Z. Fisk⁶

¹*Instituto de Física "Gleb Wataghin", UNICAMP, Campinas-SP, 13083-970, Brazil.*

²*Consejo Nacional de Investigaciones Científicas y Técnicas (CONICET)
and Centro Atómico Bariloche, S.C. de Bariloche, Río Negro, Argentina.*

³*INTEC (CONICET and UNL), S3000GLN, Santa Fe, Argentina.*

⁴*San Diego State University, San Diego, California 92182, USA.*

⁵*Department of Physics, Florida State University, Tallahassee, Florida 32306, USA*

⁶*University of California, Irvine, CA, 92697-4573, USA.*

(Dated: January 19, 2010)

Electron Spin Resonance (ESR) measurements performed on the filled skutterudite system $\text{Ce}_{1-x}\text{Yb}_x\text{Fe}_4\text{P}_{12}$ ($x \lesssim 0.003$) unequivocally reveal the coexistence of two Yb^{3+} resonances, associated with sites of considerably different occupations and temperature behaviors. Detailed analysis of the ESR data suggests a scenario where the fraction of oversized $(\text{Fe}_2\text{P}_3)_4$ cages that host Yb ions are filled with a low occupation of *on-center* Yb^{3+} sites and a highly occupied T -dependent distribution of *off-center* Yb^{3+} sites. Analysis of the $^{171}\text{Yb}^{3+}$ ($I=1/2$) isotope hyperfine splittings reveal that these two sites are associated with a low (~ 1 GHz) and a high ($\gtrsim 15$ GHz) rattling frequency, respectively. Our findings introduce Yb^{3+} in T_h symmetry systems and uses the Yb^{3+} ESR as a sensitive microscopic probe to investigate the Yb^{3+} ions dynamics.

I. INTRODUCTION

The dynamics of guest or filler ions vibrating loosely inside oversized host cages has been a topic of current focus in condensed matter physics. The anomalous behaviors of these so-called *rattler* ions raise interest both from the fundamental understanding of the unusual potential wells they are subjected to (and consequent anharmonicities in their vibrational motions) as well as from the implications of such *rattling* on the dampening of thermal transport in the material, which invites application perspectives in the field of thermoelectrics.¹ Thermoelectric materials, which can convert heat into electricity, are of great interest for energy sustainability and energy harvesting (transformation of waste heat into useful electricity). The main obstacle is the low thermoelectric efficiency of materials for heat to electricity conversion, which is quantified by the thermoelectric figure of merit, ZT . The high ZT value is the result of the high Seebeck coefficient and the low thermal conductivity.² Among the best-known cage systems displaying such characteristics are the filled skutterudite compounds RT_4X_{12} , where R is a rare earth or actinide, T is a transition metal (Fe, Ru, Os) and X is a pnictogen (P, As, Sb). Besides exhibiting a rich variety of ground states and promising thermoelectricity,³ the question of whether the R ions in these compounds are sited *on-* and/or *off-center* in the oversized rigid $(\text{T}_2\text{X}_3)_4$ -cages is a matter of intense debate.^{4,5} There is also controversy over the extent to which the weakly bounded R ions can be regarded as independent Einstein oscillators, and how effectively they contribute to a phonon-glass type of heat conduction.⁶⁻⁸ In this work we take advantage of a uniquely favorable conjunction between the chemical and structural characteristics of skutterudites and their effect on the Electron Spin Resonance (ESR) of the $J = 7/2$ multiplet of Yb^{3+} ,

to probe this ion's dynamical behavior within oversized cages of the $\text{Ce}_{1-x}\text{Yb}_x\text{Fe}_4\text{P}_{12}$ system ($x \lesssim 0.003$).

Skutterudites crystallize in the cubic $\text{LaFe}_4\text{P}_{12}$ structure with space group $Im\bar{3}$.⁹ Each R ion is surrounded by eight transition metal ions forming a cube, and twelve pnictogen ions that form a slightly deformed icosahedron. Our work lies in the fact that the local point symmetry for the R ions is T_h , which lacks two symmetry operations (C_4 and C'_2 rotations)¹⁰ when compared to common cubic structures. Thus, the electric crystal field (CF) Hamiltonian (H_{CF}) allows for an additional sixth order term with an extra crystal field parameter (CFP), B_6^t .^{11,12} This systems present a complex magnetic behavior, and it is essential to know their CF level schemes for its complete description.^{13,14}

ESR is a powerful microscopic tool to provide information about CF effects, site symmetries, valencies of the paramagnetic ions, g -values, fine and hyperfine parameters.¹² The ESR of excited states may be also observable, then, by measuring a R-ion ESR at different frequencies and temperatures, one may obtain CF ground states and, in some cases, the full set of CFP's that determine the overall splitting of a R-ion J -multiplet ground state.¹⁵ Previous works on $\text{Ce}_{1-x}\text{R}_x\text{Fe}_4\text{P}_{12}$ for R = Nd, Dy, Er, Yb; ($x \lesssim 0.005$) succeeded in explaining the low- T ESR results using such an expanded H_{CF} , and the full set of CFP's could be determined.¹⁵ However, we now found that in the case of R = Yb, as T increases, a second Yb^{3+} resonance emerges from the low- T spectra, corresponding to a distinct site, coexisting with the first one. The presence of the new term in the H_{CF} has proven essential to explain the appearance of this second Yb^{3+} resonance. The sensitivity of Yb^{3+} $4f$ -electrons to this type of CF environment make it a rare and useful probing ion to help the understanding of the potential well responsible for its motion.

II. EXPERIMENTAL

Single crystals of $\text{Ce}_{1-x}\text{Yb}_x\text{Fe}_4\text{P}_{12}$ ($x \lesssim 0.003$) were grown in Sn-flux as described in Ref. 16. The cubic structure ($Im\bar{3}$) and phase purity were checked by x-ray powder diffraction. The Yb concentrations were determined from the H and T -dependence of the magnetization, $M(H, T)$, measured in a SQUID *dc*-magnetometer. The ESR experiments used crystals of $\sim 2 \times 2 \times 2 \text{ mm}^3$ of naturally grown crystallographic faces, as well as crystals crushed into fine powder. The ESR spectra were taken in Bruker X (9.48 GHz) and Q (34.4 GHz) band spectrometers using appropriate resonators coupled to a T -controller of a helium gas flux system for $4.2 \lesssim T \lesssim 45 \text{ K}$. The ESR spectra of the $^{170}\text{Yb}^{3+}$ ($I=0$) isotope showed the superposition of a *narrow line* and a slightly shifted *broad line*. For single crystals and powdered samples the spectra were, respectively, fitted by the superposition of two dysonian (metallic lineshape) and two lorentzian resonances with adjustable resonance fields (H_0), linewidths (ΔH), A/B ratios and amplitudes.¹⁷

III. EXPERIMENTAL RESULTS

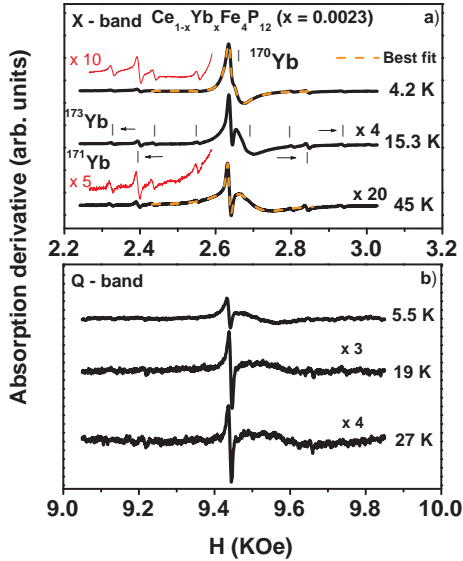


Figure 1: (color online) T -evolution ($4.2 \lesssim T \lesssim 40 \text{ K}$) of the normalized Yb^{3+} ESR spectra in a $\text{Ce}_{1-x}\text{Yb}_x\text{Fe}_4\text{P}_{12}$ ($x \approx 0.0023$) single crystal: a) X-band and b) Q-band. The enhanced low field spectra shows the absence of hyperfine lines for the *broad line*.

Figures 1a and 1b show, respectively, selected X- and Q-band ESR spectra for the Kramers doublet ground state (KDGS) of the $^{170}\text{Yb}^{3+}$ ($I=0$) isotope in a $\text{Ce}_{1-x}\text{Yb}_x\text{Fe}_4\text{P}_{12}$ ($x \approx 0.0023$) single crystal. As T increases the nearly single line observed at low- T for the

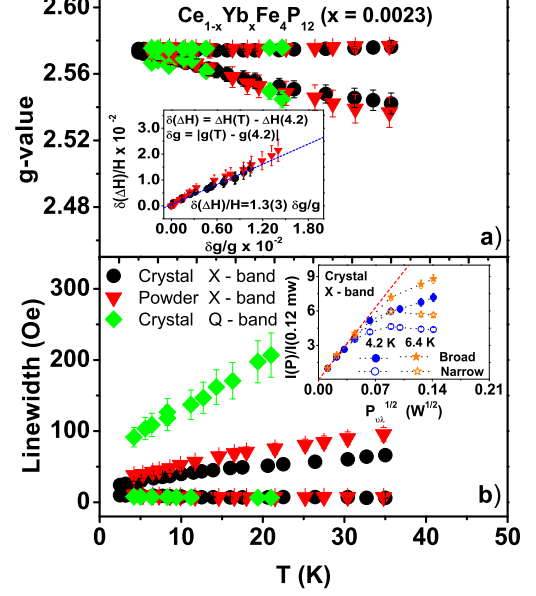


Figure 2: (color online) X and Q-bands low T -evolution of: a) g -value and b) ΔH for the *narrow* and *broad* lines of Fig. 1 and also for a powdered crystal. At X-band, Inset a) shows the correlation between $\delta(\Delta H)/H$ and $\delta g/g$, and Inset b) the microwave power dependence of the ESR intensity.

$^{170}\text{Yb}^{3+}$ isotope evolves into two lines, a *narrow* and a *broad* one. At low- T the measured g -values for the *narrow* and *broad* lines are essentially the same, $g \approx 2.57$, different from the g -values of 2.666 and 3.428 expected for Γ_6 and Γ_7 doublets, respectively.¹² At X-band the *narrow line* displays the full hyperfine spectra for the Yb isotopes $^{170}\text{Yb}^{3+}$ ($I=0$), $^{171}\text{Yb}^{3+}$ ($I=1/2$) and $^{173}\text{Yb}^{3+}$ ($I=5/2$), confirming that the observed spectra are associated to Yb^{3+} ions. From the hyperfine splittings the corresponding hyperfine constants $^{171}A = 440(10) \text{ Oe}$ and $^{173}A = 120(3) \text{ Oe}$ were obtained. These values are $\sim 20\%$ smaller than the hyperfine constants of Yb^{3+} in a KDGS of any system with O_h cubic point symmetry.^{12,18} The hyperfine lines corresponding to the *broad line* of the $^{171}\text{Yb}^{3+}$ isotope were not observed.

Figures 2a and 2b show, respectively, the T -evolution ($4.2 \lesssim T \lesssim 40 \text{ K}$) of the g -values and linewidths, ΔH , for the *narrow* and *broad* lines of Fig. 1 and also for a powdered sample at X-band. The following features are noteworthy: a) for the sites corresponding to the *narrow line* the g -value and ΔH are frequency- and T -independent; b) for the *broad line* sites the g -value and ΔH are T -dependent, and only ΔH is frequency dependent; c) the *broad line* of the powdered sample is broader than that of the crystal, while the *narrow line* is about the same; d) angular dependent ESR experiments found these resonances to be isotropic; e) for the various samples the relative change of the *broad line* linewidth, $\delta(\Delta H)/H$,

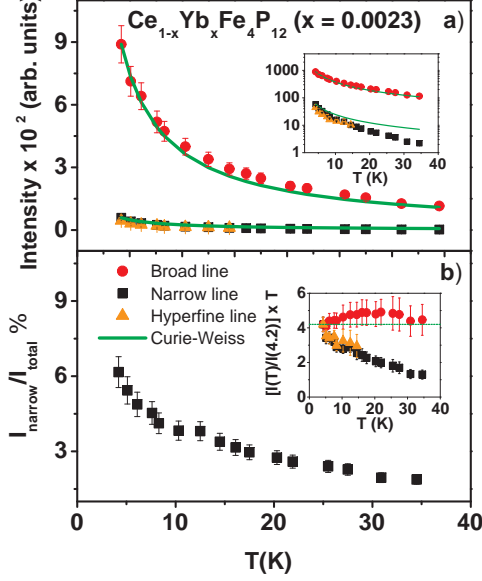


Figure 3: a) T -dependence of the ESR intensity for the two resonances of the $^{170}\text{Yb}^{3+}$ ($I=0$) isotope. The intensity of one of the $^{171}\text{Yb}^{3+}$ ($I=1/2$) hyperfine line, normalized by the natural abundance, is also shown. The inset presents the same data in log scale. b) T -dependence of the relative intensity for the *narrow line*. The inset displays the data of Fig. 3a ($\times T$) normalized at 4.2 K. The green lines show the C-W behavior.

scales at all- T with the relative change of its g -value, $\delta g/g$ ($\delta(\Delta H)/H \simeq 1.3(3) \delta g/g$, see inset of Fig. 2a); f) saturation ESR intensity measurements show that at 4.2 K and ~ 10 mW the *broad* and *narrow lines* present, respectively, a $\sim 30\%$ and $\sim 50\%$ saturation (see inset of Fig. 2b).

All the experimental features given in Figs. 1 and 2 were confirmed in crystals from different batches with comparable Yb concentrations. They lead us to conclude that: *i*) the *narrow* and the *broad lines* are, respectively, homogeneous and inhomogeneous resonances; *ii*) the origin of the inhomogeneity is a distribution of g -values of the order of the change in the g -value; *iii*) the T -independent ΔH for the *narrow line* indicates that there is no Yb^{3+} spin-lattice relaxation via exchange interaction with the conduction-electrons;^{19,20} *iv*) the saturation of the spectra at low- T suggests slow spin-lattice relaxation involving lattice phonons via spin-orbit coupling;¹² and *v*) at low- T the Yb^{3+} ions behave as an *adiabatic* spin system allowing the formation of Einstein oscillators inside the $(\text{Fe}_2\text{P}_3)_4$ -cages.

Figure 3a displays the T -dependence of the unsaturated (~ 2 mW) ESR intensity for the *broad* and *narrow lines* of the $^{170}\text{Yb}^{3+}$ ($I=0$) isotope of Fig. 1a. The intensity of one of the $^{171}\text{Yb}^{3+}$ ($I=1/2$) isotope hyperfine lines, normalized by its natural abundance, is also shown. The inset shows the data in a log scale. From their rela-

tive intensities the *broad* and *narrow lines* correspond, respectively, to $\sim 95\%$ and $\sim 5\%$ of the Yb^{3+} ions filling cages. Figure 3b presents the T -dependence of the relative population for the low occupied sites (*narrow line*). The large observed drop strongly suggests that, as T -increases, the low populated Yb^{3+} sites migrate, in a reversible way, to the highly populated Yb^{3+} ones. The inset of Fig. 3b shows for the *broad*, *narrow* and hyperfine lines the T -dependence of their intensities ($\times T$) normalized at $T \simeq 4.2$ K. This data reveals that the *broad line* practically follows a Curie-Weiss (C-W) law, while the *narrow line* surprisingly drops faster than a C-W behavior, given further support to the sites migration idea. The C-W behavior is another indication that the $^{170}\text{Yb}^{3+}$ ions carry localized magnetic moment and that the resonances arise from a CF KDGS.

IV. ANALYSIS AND DISCUSSION

In order to analyze our ESR data in Ref. 15 we used the expanded Hamiltonian, H_{CFZ} :

$$H_{CFZ} = W \left\{ (1 - |y|) \left[x \frac{O_4^c}{F_4^0} + (1 - |x|) \frac{O_6^c}{F_6^0} \right] + y \frac{O_6^t}{F_6^2} \right\} + g_J \mu_B \mathbf{H} \cdot \mathbf{J}, \quad (1)$$

where a magnetic moment \mathbf{J} with a Landé g -factor g_J is considered. The CF includes the usual cubic O_h ²¹ terms parametrized by the x variable that measures the relative weight of the 4th and 6th order terms and also takes into consideration the new term O_6^t . The relative weight y linearly interpolates between the O_h cubic terms for $y=0$ and the O_6^t term for $y=1$. This (x,y) parametrization allows the entire range of the CFP's to be accounted for within the finite intervals $-1 \leq x \leq 1$ and $|y| < 1$ and the results do not depend on the sign of y . By diagonalizing H_{CFZ} one obtains, as a function of x and y , the CF wave functions and energies for each of the R in units of W . From the ground state wave function the low field g -value can be calculated¹⁵.

A combined analysis of the ESR data for Er^{3+} , Dy^{3+} and Yb^{3+} impurities in $\text{Ce}_{1-x}\text{R}_x\text{Fe}_4\text{P}_{12}$ allowed us to pinpoint the exact $(x=0.523, y=0.082)$ values corresponding to the Yb^{3+} *narrow line* observed at $T \simeq 4.2$ K and $g \simeq 2.575$.¹⁵ However, as T increases, a second Yb^{3+} *broad line* emerges from the low- T *narrow line* (Fig. 1) and its g -value decreases, reaching $g = 2.54(1)$ at our highest- T ($\simeq 45$ K). Therefore, these two resonances should be associated to two coexisting Yb^{3+} sites with different peculiarities.

In these compounds the R-ions are known to rattle at frequencies of $\sim 10^3$ GHz⁶⁻⁸ which are low compared to the cage ion vibrations, but still much higher than the ESR frequencies (~ 10 -30 GHz). Thus, we argue that the reduced hyperfine constant for the homogeneous *narrow line* spectra results from a motional narrowing

mechanism²² of *on-center* Yb^{3+} ions rattling in the rigid oversized ($\phi \simeq 5 \text{ \AA}$) $(\text{Fe}_2\text{P}_3)_4$ -cages.⁹ In the extreme motional narrowing regime²³ a rattling frequency of $\sim 1 \text{ GHz}$ will reduce in $\sim 20\%$ the hyperfine constant. Moreover, the hyperfine structure in the inhomogeneous *broad line* spectra was not observed, suggesting that a distribution of Yb^{3+} ions are rattling at higher frequencies and producing an even larger reduction of the hyperfine constant. Again, in the extreme motional narrowing regime, a rattling frequency $\gtrsim 15 \text{ GHz}$ will reduce in 90 to 95% the hyperfine splitting, and the ESR spectra would look like the observed single *broad line* of $\Delta H \simeq 30\text{-}40 \text{ Oe}$. We should mention that the reported rattling amplitudes are $\lesssim 0.1 \text{ \AA}$.²⁴ Hence, the *broad line* T -dependent shift and broadening is most likely the result of a T -dependent distribution of Yb^{3+} ions rattling at higher frequencies inside the $(\text{Fe}_2\text{P}_3)_4$ -cages. Thus, we associate the homogeneous *narrow line*, corresponding to the low occupied sites, to *on-center* ($g = 2.575$) of $\simeq 1 \text{ GHz}$ rattling Yb^{3+} ions at ($x=0.523, y=0.082$), whereas the inhomogeneous *broad line*, corresponding to the highly occupied sites with lower g -values, to a distribution of $\gtrsim 15 \text{ GHz}$ rattling Yb^{3+} ions. Since this *broad line* is an inhomogeneous resonance (distribution of g -values) and the rattling frequency is of the order of or higher than the ESR frequency, the rattling Yb^{3+} ions responsible for these spectra should be spending more time at *off-center* positions in the over-size cage.

Since no emerging second resonance was observed from the low- T ESR spectra of Er^{3+} and Dy^{3+} ions diluted in $\text{Ce}_{1-x}\text{R}_x\text{Fe}_4\text{P}_{12}$,¹⁵ it is possible that for Yb^{3+} , with smaller ionic radius than that of Er^{3+} and Dy^{3+} , larger voided excursion space may be available for the Yb^{3+} ions inside the $(\text{Fe}_2\text{P}_3)_4$ -cages which may further favor the Yb^{3+} to rattle. A T -dependent distribution of CFPs, that in this T_h symmetry allows for a continuous change on g_{eff} ²⁵, or even a distribution of new 2^{nd} order CFPs in H_{CFZ} associated to the *off-center* Yb^{3+} sites may be also a plausible reason for the observed T -dependence of the inhomogeneous *broad line*.

V. CONCLUSIONS

In summary, our ESR results have shown that the origin for the large g -shift of the Yb^{3+} KDGS, relative to that in O_h symmetry ($y = 0$), may be associated to the $B_6^t(O_6^2 - O_6^6)$ term in H_{CFZ} . Coexisting *narrow* and *broad* Yb^{3+} resonances were observed and associated, respectively, to a low occupation ($\sim 5\%$) of *on-center* Yb^{3+} rattling ions ($\sim 1 \text{ GHz}$) and to a highly occupied ($\sim 95\%$) T -dependent distribution of *off-center* rattling Yb^{3+} ions ($\gtrsim 15 \text{ GHz}$). These assignments were based on: *i*) the much higher expected Yb^{3+} rattling frequencies than the microwave frequency used in the ESR experiments⁶⁻⁸ and; *ii*) on the observed reduction of the hyperfine constant for the *on-center* Yb^{3+} ions and the absence of hyperfine structure in the spectra of the *off-center* Yb^{3+} ions which were attributed to motional narrowing effects.^{22,23} Although our findings relied on the Yb^{3+} ESR results to witness the Yb^{3+} rattling mode, they suggest that the R ions in other skutterudites and clathrate compounds may be also rattling in an analogous form as long as they are inside an oversized cage. However, it may not be always observable in an ESR experiment. We believe that the evidence for predominant *off-center* rattling Yb^{3+} ions in these skutterudites is a result that could justify the existence of Einstein oscillators and help to understand the low thermal conductivity and the strongly correlated phenomena exhibited by these type of materials.

VI. ACKNOWLEDGMENTS

We thank FAPESP-SP and CNPq for financial support. PS is supported by DOE grant No. DE-FG02-98ER45707.

- ¹ G. J. Snyder and E. S. Toberer, Nature Mat. **7**, 105 (2008).
- ² G. Nolas and G. Slack, American Scientist **89**, 136 (2001).
- ³ See, for example, the Skutterudite2007 conference proceedings at <http://jpsj.ipap.jp/journal/JPSJS-77SA.html>
- ⁴ T. Yanagisawa, P.-C. Ho, W. M. Yuhasz, M. B. Maple, Y. Yasumoto, H. Watanabe, Y. Nemoto and T. Goto, J. Phys. Soc. Jpn. **77** 074607 (2008).
- ⁵ T. Goto, Y. Nemoto, K. Sakai, T. Yamaguchi, M. Akatsu, T. Yanagisawa, H. Hazama, K. Onuki, H. Sugawara and H. Sato, Phys. Rev. B **69**, 180511(R) (2004).
- ⁶ C. H. Lee, I. Hase, H. Sugawara, H. Yoshizawa and H. Sato, J. Phys. Soc. Jpn. **75** 123602 (2006).
- ⁷ C. B. Vining, Nature Mat. **7**, 765 (2008).
- ⁸ M. M. Koza, M. R. Johnson, R. Viennois, H. Mutka, L. Girard and D. Ravot, Nature Materials, Articles, Advance online Publication, doi: 10.1038/nmat 2260, 31 August

- 2008.
- ⁹ W. Jeitschko and D. Braun, Acta Crystallogr. B **33**, 3401 (1977).
- ¹⁰ T. Inui, Y. Tanabe and Y. Onodera, *Group Theory and its Applications in Physics* (Springer, Berlin, 1966).
- ¹¹ K. Takegahara, H. Harima and A. Yanase, J. Phys. Soc. Japan, **70**, 1190 (2001).
- ¹² A. Abragam and B. Bleaney, *EPR of Transition Ions* (Clarendon Press, Oxford, 1970).
- ¹³ Y. Nakanishi, T. Kumagai, M. Oikawa, T. Tanizawa, and M. Yoshizawa, H. Sugawara and H. Sato, Phys. Rev. B **75**, 134411 (2007); T. Yanagisawa et al., J. Magn. Magn. Mater., **310**, 223 (2007); W. M. Yuhasz, N. A. Frederick, P.-C. Ho, N. P. Butch, B. J. Taylor, T. A. Sayles, M. B. Maple, J. B. Betts, A. H. Lacerda, P. Rogl, and G. Giester, Phys. Rev. B **71**, 104402, (2005); C. R. Rotundu, K. In-

- gersent, and B. Andracka, Phys. Rev. B **75**, 104504 (2007); W M Yuhasz, P-C Ho, T A Sayles, T Yanagisawa, N A Frederick, M B Maple, P Rogl and G Giester, J. Phys.: Cond. Matt., **19**, 076212 (2007); C.. P Yang, H. Wang and K. Iwasa, Appl. Phys. Lett. **89**, 082508, (2006).
- ¹⁴ E. A. Goremychkin, R. Osborn, E. D. Bauer, M. B. Maple, N. A. Frederick, W. M. Yuhasz, F. M. Woodward, and J. W. Lynn, Phys. Rev. Lett. **93**, 157003 (2004).
- ¹⁵ D. J. Garcia, F. A. Garcia, J. G. S. Duque, P. G. Pagliuso, C. Rettori, P. Schlottmann, M. S. Torikaschvili and S. B. Oseroff, Phys. Rev. B **78**, 174428 (2008).
- ¹⁶ G. P. Meisner, M. S. Torikachvili, K. N. Yang, M. B. Maple and R. P. Guertin, J. Appl. Phys. **57**, 3073 (1985).
- ¹⁷ G. Feher and A. F. Kip, Phys. Rev. **98**, 337 (1955); F. J. Dyson, Phys. Rev. **98**, 349 (1955); G. E. Pake and E. M. Purcell, Phys. Rev. **74**, 1184 (1948).
- ¹⁸ E. P. Chock, D. Davidov, R. Orbach, C. Rettori and L. J. Tao, Phys. Rev. B **5**, 2735 (1972).
- ¹⁹ J. Korrington, Physica **16**, 601 (1950); H. Hasegawa, Prog. Theor. Phys. (Kyoto) **21**, 1093 (1959).
- ²⁰ C. Rettori, D. Davidov, R. Orbach, E. P. Chock and B. Ricks, Phys. Rev. B **7**, 1 (1973).
- ²¹ K. R. Lea, M. J. M. Leask and W. P. Wolf, J. Phys. Chem. Solids **23**, 1381 (1962).
- ²² H. A. Farach, E. F. Strother and C. P. Poole, J. Phys. Chem. Solids **31**, 1491 (1970).
- ²³ P. W. Anderson, J. Phys. Soc. of Japan **9**, 316 (1954).
- ²⁴ D. Cao, F. Bridges, P. Chesler, S. Bushart, E. D. Bauer and M. B. Maple, Phys. Rev. B **70**, 094109 (2004).
- ²⁵ F. A. Garcia, D. J. Garcia, J. G. S. Duque, P. G. Pagliuso, C. Rettori, P. Schlottmann, M. S. Torikachvili and S. B. Oseroff, Accepted in Phys. B 2009.